Toward a plasma-based accelerator at high beam energy with high beam charge and high beam quality

P. A. P. Nghiem[1,*] R. Assmann,[2a] A. Beck,[3] A. Chancé,[1] E. Chiadroni,[4] B. Cros,[5]
M. Ferrario,[4] A. Ferran Pousa,[2a,2b] A. Giribono,[4] L. A. Gizzi,[6] B. Hidding,[7] P. Lee,[5] X. Li,[8]
A. Marocchino,[9] A. Martinez de la Ossa,[2a] F. Massimo,[3] G. Maynard,[5] A. Mosnier,[1] S. Romeo,[4]
A. R. Rossi,[10] T. Silva,[11] E. Svystun,[2a] P. Tomassini,[6] C. Vaccarezza,[4] J. Vieira,[11] and J. Zhu[2a]

[1]*CEA, IRFU, Université Paris Saclay, F-91191 Gif-sur-Yvette, France*
[2a]*Deutsches Elektronen-Synchrotron, 22607 Hamburg, Germany*
[2b]*Institut für Experimentalphysik, Universität Hamburg, 22761 Hamburg, Germany*
[3]*CNRS, LLR, Ecole Polytechnique, 91128 Palaiseau, France*
[4]*INFN, Laboratori Nazionali di Frascati, 00044 Frascati, Rome, Italy*
[5]*CNRS, LPGP, Université Paris-Sud, Université Paris-Saclay, 91405 Orsay, France*
[6]*CNR Istituto Nazionale di Ottica, 56124 Pisa, Italy*
[7]*Cockcroft Institute, Warrington WA4 4AD, United Kingdom*
[8]*Deutsches Elektronen-Synchrotron, 15738 Zeuthen, Germany*
[9]*Sapienza, University of Rome, 00161, Rome, Italy*
[10]*INFN, Sezione di Milano, 20133 Milan, Italy*
[11]*GoLP/Instituto de Plasmas e Fusão Nuclear, Instituto Superior Técnico,
Universidade de Lisboa, 1049-001 Lisbon, Portugal*

From plasma-wakefield acceleration as a physics experiment toward a plasma-based accelerator as a user facility, the beam physics issues remaining to be solved are still numerous. Providing beams with high energy, charge, and quality simultaneously, not only within the plasma but also at the user doorstep itself, is the main concern. Despite its tremendous efficiency in particle acceleration, the wakefield displays a complex 3D profile which, associated to the beam-loading field induced by the accelerated beam itself, makes the acceleration of high charge to high energy often incompatible with high beam quality. Beam extraction from the plasma without quality degradation for a transfer either to the next plasma stage or to the user application is another difficulty to consider. This article presents the substantial studies carried out and the different innovative methods employed for tackling all these different issues. Efforts focused on achieving the challenging beam parameters targeted by the EuPRAXIA accelerator facility project. The lessons learned at the end of these in-depth simulations and optimizations are highlighted. The sensitivity to different error sources is also estimated to point out the critical components of such an accelerator. Finally, the needs in terms of laser and plasma parameters are provided.

I. INTRODUCTION

Laser or particle beams propagating in a plasma can drive an electric field several orders of magnitude more intense than that produced by radio-frequency (rf) cavities in conventional accelerators. This leads to the promise of much more compact particle accelerators. Different plasma-based acceleration and injection techniques have

been imagined, using either laser or particle beams as drivers in different acceleration regimes, from linear to strongly nonlinear (see [1,2], and references therein). Ingenious laser-plasma experiments have been set up, demonstrating first the possibility to accelerate electrons to hundreds of MeV [3,4,5], then to the symbolic threshold of 1 GeV [6], and then to 2 [7], 3 [8], 4 [9], and very recently 8 GeV [10]. These experimental results are supported by simulations with 3D particle-in-cell (PIC) codes, which further explore the acceleration up to 10 GeV [11], hundreds of GeV [12], or even 1 TeV [13], assuming the achievement of a good enough electron injection. Those experimental and theoretical results have been obtained with a certain care about either the charge or else the beam quality in terms of energy dispersion and emittance, but the latter are still far from those obtained in rf accelerators.

Recently, particular efforts have been dedicated to obtain high-quality beams, with less than 1 mm mrad emittance, less than 1% energy spread, and either a high energy gain or else a high accelerated charge [14–17].

This continuous progress in plasma-based acceleration would suggest that the era of plasma-based accelerators is coming up. However, from acceleration as a physics experiment toward an accelerator as a facility delivering a beam to users, major steps remain to be achieved. Even if we set aside questions about reproducibility or reliability and focus only on beam physics considerations, important challenges remain to be solved. An accelerator must provide beams with high enough energy, charge, and quality, all simultaneously, and at the user doorstep itself. Until now, this has not been demonstrated or even expected for plasma-based acceleration techniques. Indeed, a higher energy gain nearly entails a lower beam quality, because the beam must be accelerated for longer distances and, consequently, experiences different regimes of the plasma wakefield. A high charge beam can lead to quality degradation, at least in linear or quasilinear acceleration, as the beam self-field (beam loading), which is nonlinear, becomes important. A whole accelerator should also have its own beam injection and extraction systems, which are the transfer lines. They should be capable of extracting the beam from a plasma stage and injecting it into the next plasma stage or delivering it to the user application with minimum quality degradation. Such a transfer line for a high charge with substantial beam loading remains to be demonstrated. Extracting the particle beam from the accelerating plasma without special precautions can lead to significant (orders of magnitude) emittance growth.

It is therefore still necessary to develop new strategies or methods of particle injection and acceleration in order to take the leap toward a plasma-based accelerator. Let us consider, for example, the ambitious objectives of the EuPRAXIA accelerator project [18]. The main requirements are summarized in Table I for the electron beam at the exit of the injector, which can be either a laser-plasma injector or a radio-frequency injector, and at the accelerator end, i.e., at the user application. These beam characteristics, suitable for a highly demanding application such as the free electron laser (FEL), are particularly challenging. They require simultaneously a high final energy of 5 GeV (with a commissioning step at 1 GeV), a high charge of 30 pC in a short length of 10 fs (i.e., a high peak current of 3 kA), a low emittance of 1 mm mrad, a low energy spread of 1%, and an even lower slice energy spread of 0.1%.

In this article, we will present and discuss the different strategies and methods that are developed aiming at meeting the above challenging requirements. In Sec. II, the injection and acceleration schemes and techniques under investigation are presented. The final beam characteristics obtained after optimization are compared to the objectives, and the down selection procedure is performed. Note that

TABLE I. Main requirements for the electron beam at the exit of the injector, which can be either a laser-plasma (LP) injector or a radio-frequency (rf) injector, and at the accelerator exit, which means at the user application. E, Q, τ(FWHM), σ_E/E, $\sigma_{E,S}/E$, ε_n, and $\varepsilon_{n,S}$ stand, respectively, for beam energy, charge, length (full width at half maximum), rms energy spread, slice energy spread, normalized phase emittance, and slice normalized phase emittance.

Parameter	LP injector exit	rf injector exit	Accelerator exit
E	150 MeV	250–500 MeV	5 GeV (1 GeV)
Q	30 pC	30 pC	30 pC
τ (FWHM)	10 fs	10 fs	10 fs
σ_E/E	5%	0.2%	1%
$\sigma_{E,S}/E$	t.b.d.	t.b.d.	0.1%
ε_n	1 mm mrad	1 mm mrad	1 mm mrad
$\varepsilon_{n,S}$	t.b.d.	t.b.d.	1 mm mrad

these results reflect the present status of our studies. They are subject to further improvements later on. In Sec. III, the lessons learned from these vast studies, the receipts how to meet all the requirements, are discussed. The necessary uncoupling of injection and acceleration is pointed out, and the methods to obtain high beam quality and charge at once are detailed. In Sec. IV, the beam extraction from a plasma stage and its transfer to the next plasma stage or toward the end application are analyzed, and then optimized, in order to mitigate the degradation of beam quality previously obtained. In Sec. V, the sensitivity to errors is estimated so as to identify the most critical components to which special care should be dedicated. In Sec. VI, the plasma and laser parameters that allowed us to meet the requirements are specified. The conclusions are summarized in Sec. VII.

II. BROAD EXPLORATION, OPTIMIZATION, AND DOWN SELECTION

A. Study of injection and acceleration schemes

One of the best ways to jump from the plasma-based acceleration as a physics experiment toward a plasma-based accelerator is to adopt a similar approach to the design of a conventional accelerator. Before fabricating and installing a conventional (rf) accelerator, a substantial design phase is always carried out. It consists first in selecting the most appropriate configuration regarding the objectives, for example, a linear or circular accelerator, room temperature or cryogenic components, etc. Then, in optimizing thoroughly the beam physics by means of simulations until the targeted beam characteristics are obtained, the parameters of all the accelerator components can be technically specified, including their tolerances.

We propose to apply the same strategy for designing a plasma-based accelerator. Yet, due to the relative youth of this field, there are three main issues: The limits of each plasma wakefield configuration or technique are much less
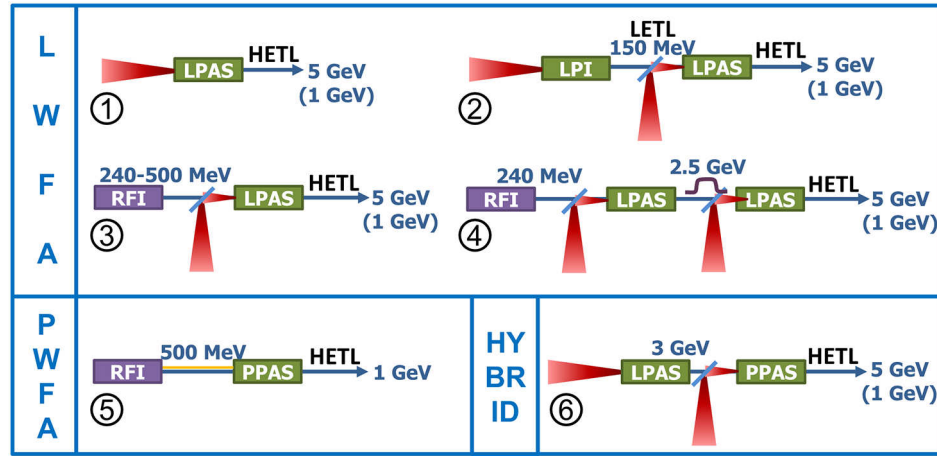
FIG. 1. The injection and acceleration schemes under investigation. RFI stands for radio-frequency injector, LPI for laser-plasma injector, LPAS for laser-plasma acceleration stage, and PPAS for particle-plasma acceleration stage. LETL and HETL stand for low-energy and high-energy transfer lines, respectively. Schemes 1–4 are related to laser-driven wakefield acceleration where the laser beam is represented in red. Scheme 5 is related to particle-driven wakefield acceleration. Scheme 6 is related to a hybrid configuration mixing laser-driven and beam-driven acceleration.

known, beam simulations are much more time consuming, and the vast number of simulation codes and their reliability could be questionable. We are thus forced to explore broadly and to down select different acceleration or injection schemes and techniques. This rather long procedure was feasible only thanks to the many contributors of the EuPRAXIA Collaboration.

In the beginning, many injection and acceleration schemes were explored, including or not external injection, followed by one or two plasma acceleration stages, for accelerating to 5 GeV directly or with an intermediate step at 1 GeV. First simulations showed that acceleration to 5 GeV is quite accessible in one acceleration stage. It is therefore not useful to consider schemes with multiple acceleration stages, since they would need transfer lines between the stages, except when longitudinal beam manipulations are revealed to be beneficial during the acceleration process so that it is useful to split it into two parts.

The studied schemes are finally reduced as sketched in Fig. 1, where the beam energy is also indicated at each stage exit. Schemes 1–4 refer to laser-driven wakefield acceleration (LWFA), where the electrons can be internally injected or else externally injected by an rf injector or a laser-plasma (LP) injector. The acceleration is performed in a single stage directly to 5 GeV, except in the fourth scheme, where this stage is split into two symmetric parts in order to install a magnetic chicane for energy dechirping. The laser considered in this article refers to the Ti:sapphire laser system operating at the 0.8 μm wavelength [19]. Scheme 5 refers to particle-driven wakefield acceleration (PWFA), where until now only the final energy of 1 GeV has been studied, with the electron bunch externally injected from a 500 MeV rf injector. Scheme 6 refers to a hybrid configuration where a first LWFA plasma stage

will provide a 3.5 GeV particle beam to drive the wakefield in a second PWFA plasma stage, accelerating witness electrons to 5 GeV.

Each injection or acceleration stage of a given scheme has been studied with different injection or acceleration techniques, leading to many different possible configurations.

B. Study of injection stages

Two different rf injectors have been optimized so as to provide 240 or 500 MeV electrons with beam quality meeting the requirements indicated in Table I.

(a) An S-band linac with successive compressions by rf and magnetic components is studied. This hybrid-compression scheme helps to reduce the nonlinearity of the longitudinal phase space. The exit energy should be the lowest for size and cost considerations, but it should be high enough to reduce space charge forces so that the required peak current and emittance can be obtained. It is shown that an electron bunch of 30 pC, 7.5 fs rms length, 0.5 μrad emittance as required can be obtained at the plasma injection point, at the condition to accelerate the beam up to the energy of 240 MeV where space charge forces are less harmful [20].

(b) Another strategy with pure rf compression based on velocity bunching [21] has been considered to produce in one stage a 100 MeV, 3 kA beam at the end of the 2.856 GHz S-band traveling wave sections [22]. An additional X-band linac configuration with accelerating gradient 60 MV/m is meant to boost the beam energy up to ~500 MeV, while the proper matching conditions at the plasma entrance are achieved with a triplet of permanent quadrupoles. For the use of PWFA, a laser-comb configuration [23,24] has been applied for producing two electron bunches, a 200 pC driver followed by a 30 pC witness

bunch. By illuminating the photocathode with a train of laser pulses with well-controlled timing, two or more electron bunches can be accelerated within the same rf accelerating bucket. The witness is created earlier than the driver on the photocathode, but their longitudinal positions are then reversed at the end of the velocity bunching process. The optimization consists in setting the parameters of the two electron bunches and the longitudinal distance between them as desired at the next plasma acceleration stage. In particular, the two bunches should be separated by at least half the plasma wavelength.

For the laser-plasma injector (LPI) providing a 150 MeV beam, five different injection techniques have been simulated and optimized.

(a) *Wave-breaking injection and acceleration in the nonlinear regime.*—The aim is to produce electron self-injection only at the early stage of laser pulse propagation, followed by its stable self-guiding so as to prevent continuous self-injection of background electrons. With the laser and plasma parameters resulting from the studies described in Ref. [25] and reported in Table II, simulations with the PIC code SMILEI [26] show that, with a powerful laser, a very big charge of 1 nC is self-injected and then accelerated to 204 MeV after only 1.35 mm propagation. However, the resulting 7 mm mrad emittance and 15% energy spread are well larger than the requirements of Table I. This technique is suitable for injecting a big charge and accelerating it to energies up to 1 GeV, but the output beam quality is generally modest.

(b) *Shock-front injection and acceleration in the bubble regime.*—The principle is to focus the laser beam on a plasma density plateau with, in front of it, a steep up and down ramp of ~100 μm length [27]. Systematic variations of the density-transition parameters have been explored. It is found that longer and lower density transitions induce less available electrons for injection and less wake bubble size increase, resulting in a lower beam loading and, thus, a negative correlation between the final beam charge and energy. Simulations with the PIC code CALDER-Circ [28] on a 200-processor calculator show that, in the laser and plasma conditions indicated in Table II, an 80 pC charge is self-injected and accelerated to more than 100 MeV with an

emittance of 1.5 mm mrad and an energy spread $\lesssim 15\%$. With this technique, the injected charge is still remarkable and the emittance is better controlled, but the energy spread is well higher than required.

(c) *Ionization injection and acceleration in the nonlinear regime.*—This study is based on an experimental setup composed of a 5-mm-long gas cell equipped at the two ends with variable length tubes of smaller radius allowing one to adjust the plasma ramps [29]. The cell is filled with hydrogen gas containing impurities of high-Z nitrogen. The combined variations of the nitrogen concentration and the density length and ramps allow one to adjust the beam-loading effect and the accelerating field profile so as to optimize the beam quality and the energy gain. Simulations with the 3D PIC code WARP [30] on a 1000-core calculator show that, in the laser and plasma configuration as recorded in Table II, 27 pC can be ionized and then accelerated to 142 MeV, with the energy spread $\sigma_E/E = 4\%$ and the emittances $\varepsilon_x = 0.8$, $\varepsilon_y = 1.8$ mm mrad [31]. The larger emittance in the laser polarization direction is one typical characteristic of the ionization injection.

(d) *Down-ramp injection and blowout acceleration.*—The principle is similar to that of the shock-front technique in (b), with an acceleration performed in a ~2-mm-long plasma density plateau, but preceded by a smoother and longer density step with more parameters to adjust in order to improve the beam quality at injection [32]. More details and discussions will be given in the next sections. Simulations with the 3D PIC code OSIRIS [33], in the conditions of laser and plasma as indicated in Table II, demonstrate the possibility for the output beam to meet the requirements when only the core part of the beam is considered: 30 pC charge, 255 MeV energy, 0.15 mm mrad emittance, and 0.8% energy spread. Notice that, in this configuration, the laser is self-focused and its strength a_0 is doubled inside the plasma.

(e) *Resonant multipulse ionization injection (ReMPI).*—This technique relies on gas ionization as in (c) above, but the laser pulse is here split into two (or three) components, the main one decomposed in a train of four pulses to drive the plasma wakefield, a small component in the third harmonics to ionize the gas, and, if necessary, a tiny component with perpendicular polarization to make the beam symmetrical [16,34]. The multipulse decomposition needs a more sophisticated laser configuration [35], but this allows one to obtain a high-quality beam. More details and discussions will be given in the next sections. Simulations have been performed with the ALaDyn [36] and QFluid [37] codes, the latter having been benchmarked with the FBPIC [38] code. With the laser and plasma parameters mentioned in Table II, 31 pC electrons can be injected and accelerated to 150 MeV through a 3.5-mm-long plasma of preionized nitrogen 5+, with at the exit a 0.3 mm mrad emittance and 1.7% energy spread.

TABLE II. Laser and plasma parameters of the studied injection techniques. P_L, E_L, a_{0L}, and τ_{FWHM} stand for the laser pulse power, energy, strength, and duration, respectively. n_p and l_p stand for the plasma density and length, respectively.

LPI	P_L	E_L	a_{0L}	τ_{FWHM}	n_p
(a)	353 TW	10.5 J	2.6	28 fs	5×10^{18} cm^{-3}
(b)	30 TW	0.9 J	2.5	28 fs	3×10^{18} cm^{-3}
(c)	22 TW	0.47 J	1.6	20 fs	4×10^{18} cm^{-3}
(d)	35 TW	1.05 J	1.8	30 fs	4×10^{18} cm^{-3}
(e)	200 TW	5 J	1.1	30 fs	1×10^{18} cm^{-3}

C. Study of acceleration stages

For the LWFA schemes, the acceleration stages providing a 5 GeV beam have been studied with different acceleration techniques leading to various and revealing results.

The scheme-1 laser-plasma acceleration stage (LPAS) was simulated with the ReMPI technique, with a slightly more sophisticated configuration as above, allowing obtaining 30 pC at 5 GeV with an emittance and energy spread well below the requirements. For that, the driver laser pulse must be decomposed into eight subpulses, the ionization pulse must be in the fourth harmonics, and the plasma must be split into two sections, with a gas jet for ionizing the doped gas (argon) and trapping the ionized electrons, immediately followed by a 25-cm-long capillary for acceleration [39].

The scheme-2 LPAS is studied under the quasilinear regime, with first as input the 150 MeV bi-Gaussian beam having the required parameters of Table I. Simulations have been done with the 3D PIC code WARP [30]. The laser and plasma parameters reported in Table III are defined following the scaling laws for having a resonant wakefield. The plasma depth is defined to match the laser injection. The transverse beam size is defined to minimize emittance growth [40], and the longitudinal beam size is defined to minimize the energy spread by using the beam-loading effect [41]. More detailed discussions will be given in the next sections. This thorough optimization of each of those parameters allows one to obtain the acceleration of 30 pC up to 5 GeV after 26 cm with the beam quality as required in Table I: $\varepsilon_{x,y} = 1$ mm mrad, $\sigma_E/E = 0.8\%$, slice $\varepsilon_{x,y,s} = 1$ mm mrad, $\sigma_{E,s}/E = 0.1\%$, and $\tau_{FWHM} = 7$ fs. In addition, for this LPAS, the input beam coming from the 150 MeV LPI and transferred by the optimized low-energy transfer line (LETL) has also been considered. Its parameters are about 20% different from the bi-Gaussian beam, and its shape is, of course, not bi-Gaussian. Despite that, and despite another simulation code used, FBPIC [38], a rapid retuning of the LPAS parameters following the above-mentioned principles allowed us to obtain a final beam with very close characteristics as described above.

The scheme-3 LPAS was studied considering input beams from the two different rf injectors described in the previous section.

(a) The quality degradation of the 240 MeV input beam coming from the rf injector has been estimated with respect to the plasma up-ramp length or the offset between the electron beam center and the laser beam center [42]. Subsequent optimizations with the quasi-3D code FBPIC demonstrate that, with the laser, plasma, and electron input beam parameters recorded in Table III, 20 pC can be accelerated in the quasilinear regime for 9 cm to 4.4 GeV, with the beam quality not far from required: $\varepsilon_{x,y} = 1.5$, 0.8 mm mrad, $\sigma_E/E = 1\%$, slice $\varepsilon_{x,y,s} = 0.1$ mm mrad, $\sigma_{E,s}/E = 0.1\%$, and $\tau_{FWHM} = 4.2$ fs.

(b) For the input beam coming from the 500 MeV rf injector, the same quasilinear acceleration regime is applied. The plasma target profile comprises two equal exponential input and output ramps and a constant density plateau. The ramp characteristic length is chosen to be half of the bunch betatron wavelength at injection. This length is realistic and has been shown to yield the same results, in terms of beam parameters, as longer ramps [43]. The plasma density is set so that the plasma wavelength is much longer than the beam length, in order to avoid an excessive energy spread increase, while retaining an accelerating gradient around 10 GV/m. The laser parameters are set in order to both increase the dephasing length and maximize the laser-to-plasma energy transfer. The resulting laser, plasma, and electron input beam parameters are shown in Table III. Simulations [44] have been performed with the QFluid code, a hybrid fluid-PIC tool, where the plasma is assumed to behave like a cylindrically symmetric fluid while the electron beam is treated using a full 3D PIC model. When optimizing both the injection phase and matching into the plasma channel for preservation of 6D brightness, up to 24 pC can be accelerated to 5.3 GeV after 50 cm, with very good beam quality: $\varepsilon_{x,y} = 1.5$, 0.8 mm mrad, $\sigma_E/E = 0.1\%$, slice $\varepsilon_{x,y,s} = 0.36$ mm mrad, $\sigma_{E,s}/E = 0.04\%$, and $\tau_{FWHM} = 11$ fs.

The scheme-4 LPAS was studied under the blowout regime. As previously described, the acceleration in this scheme is performed in two identical plasma stages joined by a magnetic chicane in which the bunch chirp is inverted [45]. The externally injected beam is coming from the 250 MeV rf injector described above. It should be noted, however, that a certain smoothing was applied to the

TABLE III. Laser and electron input beam parameters of the LWFA LPAS. The plasma density is $n_p = 1$. 10^{17} cm^{-3} for all the LPAS cases. The same notations as for Table II.

LPAS	Laser beam				Electron input beam			
	P_L	E_L	a_{0L}	τ_{FWHM}	E	$\varepsilon_{x,y}$	σ_E/E	τ_{FWHM}
Sch1	872 TW	51 J	0.64	55 fs	$\cdots$	$\cdots$	$\cdots$	$\cdots$
Sch2	341 TW	45 J	2.00	132 fs	150 MeV	1.0 μ	0.5%	7.0 fs
Sch3 a)	320 TW	37 J	1.95	120 fs	240 MeV	0.8, 0.5 μ	0.11%	17.8 fs
Sch3 b)	225 TW	25 J	1.15	110 fs	540 MeV	0.4 μ	0.06%	11.0 fs
Sch4	750 TW	40 J	3.00	50 fs	250 MeV	0.5 μ	0.5%	4.5 fs

current profile to emulate the effect of a laser heater in the bunch compressor and prevent the onset of micro-bunching in the chicane between LPAS. The initial parameters of this electron beam and of the laser drivers are given in Table III. The plasma cells feature a density plateau of 8 cm with a transverse parabolic profile for laser guiding. In addition, plasma-to-vacuum transitions (plasma ramps) following the expression $n_{p,\mathrm{ramp}} = n_p/(1 + z/L_r)^2$ have been considered. This ramp shape, where $n_p = 10^{17}$ cm^{-3} is the plateau density, z is the distance to the plateau, and L_r determines the density gradient, has been found to provide good performance for matching and emittance preservation [46]. The plasma stages are separated by a distance of 3.4 m, where the transport line with the chicane is placed. The chicane is composed of four 20-cm-long dipoles with a 0.4 T field providing a 7.8 mrad bending angle. Two active plasma lenses, placed at 30 cm away from the plasma stages, as well as two quadrupole doublets are used for the beam transport. The plasma simulations (including accelerating stages and plasma lenses) were performed with FBPIC, while the tracking codes ASTRA [47] and CSRTRACK [48] were used for the transport line. By properly tailoring the plasma ramps and the beam transport, 23.7 pC can be accelerated to a final energy of 6 GeV with high beam quality: $\varepsilon_{n,x} = 1.5$ mm mrad, $\varepsilon_{n,y} = 0.7$ mm mrad, $\sigma_E/E = 0.41\%$, slice $\varepsilon_{n,x,s} = 0.77$, $\varepsilon_{n,y,s} = 0.4$ mm mrad, $\sigma_{E,s}/E = 0.054\%$, $\tau_{\mathrm{FWHM}} = 3.1$ fs, and $I_{\mathrm{peak}} = 4.9$ kA.

For the PWFA (scheme 5), the two rf injectors necessary for obtaining the final energies 1 or 5 GeV will be very different, so it is decided in a first step to study only the first case. The objective is to accelerate the bunch from 540 MeV to 1 GeV without phase-space dilution in the weakly nonlinear regime, characterized by a wakefield departing from a sinusoidal wave, tending toward a sawtooth profile. In order to minimize the energy spread, the beam-loading effect is used to compensate the energy chirp, by means of a longitudinally triangular-shape wit-ness beam, injected 184 μm behind the driver beam and at a position in the bubble so that there is enough room for the bunch transverse extension. In these conditions, the accel-erated field experienced is 1.1 GV/m. Simulations have been performed with the Architect code [49,50], where the electron bunch is treated in 3D PIC and the plasma background in cylindrical fluid. With the beam parameters at the entrance as indicated in Table IV, 40 pC charge can be accelerated to 1 GeV after 40-cm-long plasma at 1.0×10^{16} cm^{-3} density contained in a capillary. The electron beam at the exit has a good quality as required: $\varepsilon_{x,y} = 0.9$ mm mrad, $\sigma_E/E = 1.2\%$, slice $\varepsilon_{x,y,s} = 1.2$ mm mrad, $\sigma_{E,s}/E = 0.036\%$, and $\tau_{\mathrm{FWHM}} = 12$ fs.

The hybrid scheme 5 is studied with two different injection techniques: the wakefield ionization injection (WII) and the Trojan horse injection (THI).

TABLE IV. Beam parameters at the plasma entrance for scheme 4A (PWFA).

	E	$\varepsilon_{x,y}$	σ_E/E	τ_{FWHM}
Driver beam	540 MeV	3 mm mrad	0.1%	313 fs
Witness beam	540 MeV	0.9 mm mrad	0.06%	12 fs

The WII configuration is based on two plasma stages [51]. The first one is a LPAS whose mission is to provide a driver beam to the second one, a PPAS (see Fig. 1). By upscaling by a factor of 10 the results obtained from simulations with the 3D PIC code OSIRIS [33], one can assume that with the laser and plasma parameters P = 980 TW, E = 88 J, $a_0 = 3.18$, $n_p = 2 \times 10^{17}$ cm^{-3}, and the ionization injection followed by an acceleration in the bubble regime, a very high charge, high energy electron beam can be generated at the LPAS exit: Q = 600 pC, E = 3.7 GeV, $\varepsilon_{x,y} = 15$ mm mrad, $\sigma_E/E = 2.5\%$, and $\tau_{\mathrm{FWHM}} = 19$ fs. As its peak current is high enough (>8.5 kA) and its duration is comparable to the plasma wavelength, its injection into the PPAS will drive a strong wakefield, ready for accelerating witness electrons, again in the bubble regime. The same wakefield presents a location where its amplitude combined with an optimized dopant gas concentration allows electron injection with a very high beam quality [52]. Note that it is imperative to properly adjust the beam-loading field and to make so that the charge injection is restricted to a small phase-space area at the back of the first plasma bucket. Simulations show that acceleration through a high-density 2×10^{19} cm^{-3}, 1.2-cm-long plasma allows to obtain an ultrahigh brightness beam at the required energy but with a relatively high energy spread and low charge: Q = 11 pC, E = 5 GeV, $\varepsilon_{x,y} = 0.16$ mm mrad, $\sigma_E/E = 3\%$, slice $\varepsilon_{x,y,s} = 0.25$ mm mrad, $\sigma_{E,s}/E = 0.25\%$, and $\tau_{\mathrm{FWHM}} = 0.8$ fs.

A conceptual design has been done for the THI con-figuration. The idea is to use the Trojan horse injection technique to reduce the transverse beam emittance [14] and a supplementary escort beam to reduce the energy spread [53]. A PPAS containing a H2/He gas mixture is considered, fed by an upstream LPAS and a 10 GW laser beam. The latter ionizes the H2 gas to generate the witness beam. The LPAS, itself fed by two laser beams, provides (i) a driver beam that ionizes the He gas by means of its self-field and simultaneously generates a blowout acceleration regime and (ii) a large-size escort beam at the location where the witness beam already reaches a high enough relativistic energy. The role of the escort beam is to flatten the local field via the beam-loading effect, without deteriorating the witness beam emittance. It should be also easily separable from the witness beam. For that, the escort bunch must overlap the witness bunch, with a significantly higher charge and lower energy. Simulations have been performed with the 3D PIC code VSim [54]. Assuming the availability of an ionization injection laser with P = 10 GW,

$E = 0.2$ mJ, $a_0 = 0.018$, $w_0 = 7$ μm, and $\tau_{\text{FWHM}} = 25$ fs, it is found that, after 5 cm propagation in a 1.1×10^{17} cm^{-3} plasma, a 9 pC witness beam can be accelerated to 5 GeV with $\varepsilon_{x,y} = 0.05$ mm mrad, $\sigma_E/E = 0.05\%$, slice $\varepsilon_{x,y,s} = 0.04$ mm mrad, $\sigma_{E,s}/E = 0.03\%$, and $\tau_{\text{FWHM}} = 1$ fs. The energy is high enough, the beam quality is remarkable, while the charge is relatively low, but there is still room for improvement.

D. Selection of the most suitable configurations

The beam parameters obtained in the previous section at the exit of the 150 MeV LPI are sketched in Fig. 2, where they are compared to the requirements. Among the five different injection techniques applied, the wave-breaking and shock-front injections are more appropriate for obtaining a very big charge than a good beam quality. With the ionization technique, results are not very far from the requirements, while the ReMPI and down-ramp techniques completely met the requirements. As such, the two last techniques can be considered as the most suitable for the present requirements. They will be discussed in more detail in the next sections.

The results obtained by the different acceleration techniques up to 5 GeV are gathered and compared to the requirements in Fig. 3 (the good results obtained by the PWFA technique is not considered here, as it was studied only for acceleration up to 1 GeV). We can see that the four LWFA schemes with external injection all exhibit results closer to the requirements (especially three of them practically meet all the requirements), with nevertheless
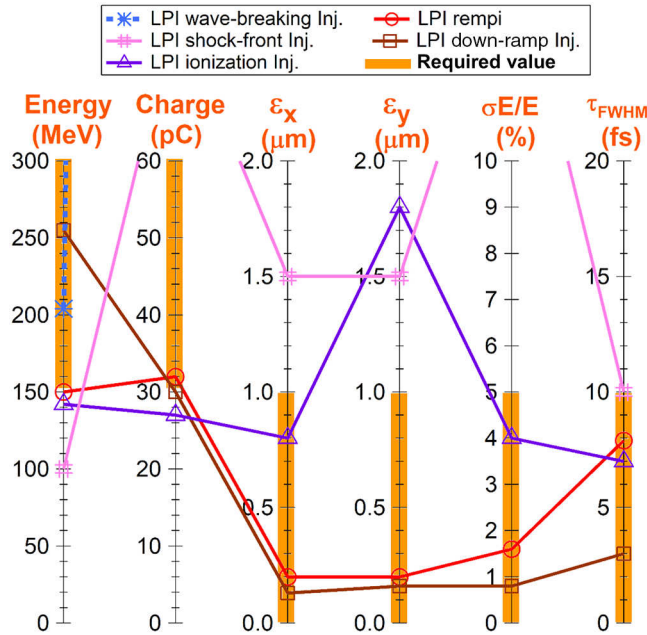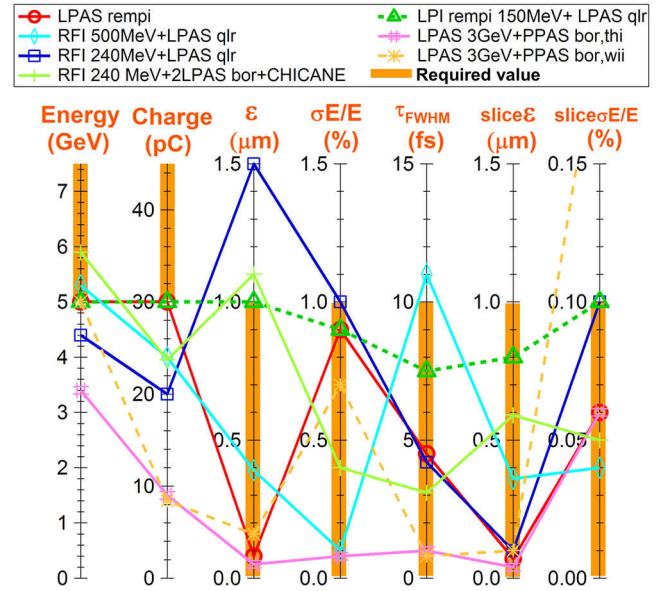

FIG. 3. Beam parameters obtained at the 5 GeV LPAS exit compared to the requirements for seven different acceleration techniques and beam injections. qlr and bor stand for, respectively, quasilinear regime and blowout regime.

a weak margin. It is also important to highlight the results obtained with the acceleration in the quasilinear regime, which are performed in four different institutes, with three different codes (3DPIC WARP, quasi-3D FBPIC, and QFluid) built following completely different basis. Despite that and despite the use of four different input beams at different energies (this will affect only the acceleration length), when the laser and plasma parameters are close as seen in Table III, the beam at the LPAS exit can feature similar characteristics. This means that the simulation codes are consistent between them, at least for these three codes and for the quasilinear regime, but above all, the results thereby obtained present a strong robustness. This is very encouraging: Not only is there an acceleration configuration that can provide results meeting all the EuPRAXIA requirements, the quasilinear acceleration with external injection, but in addition it is robust, in the sense that moderate variations of the input parameters will demand only moderate retuning to obtain the required accelerated beam.

It is important to keep in mind that all the results shown here simply give the present status of our studies. Further optimizations under consideration could still lead to significant improvements.

The above-discussed parameters refer to the first and second moments of the particle distribution in order to characterize it the most concisely as possible. A more extensive way to describe it is to present its projections onto different phase spaces. An example is given in Fig. 4 for the 5 GeV beam at the exit of the scheme-2 LPAS, after 26 cm acceleration in the quasilinear regime of the 150 MeV input beam coming from the ReMPI injector that has been transferred by the related LETL.
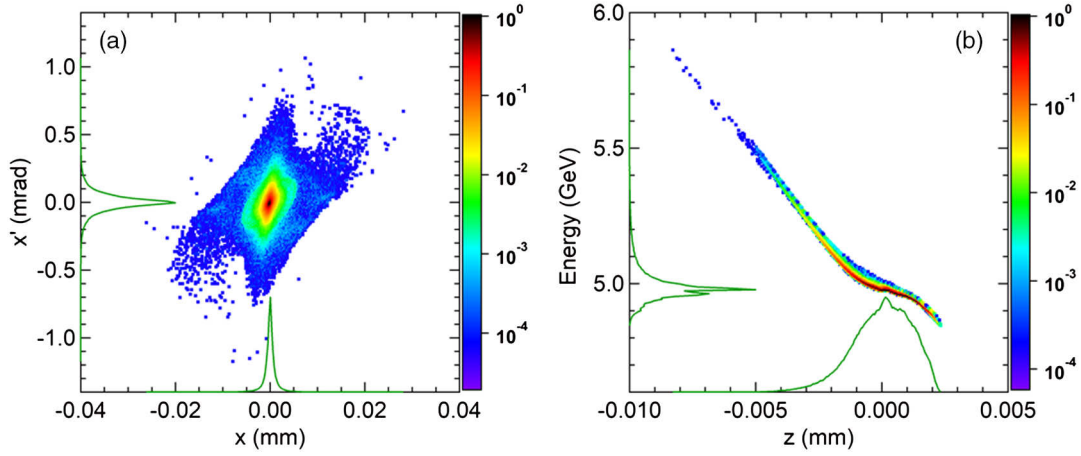

FIG. 2. Beam parameters obtained at the 150 MeV LPI exit compared to the requirements for five different injection techniques.

FIG. 4.   Beam density distribution at the exit of the scheme-2 LPAS (see the text), for 500000 macroparticles. (a) Projection onto the phase space (x, x′), i.e., transverse position and angle. (b) Projection onto (z, E), i.e., longitudinal position and energy. The color bar on the right represents the density scale normalized to 1. The green lines on the axes are the projections onto the axes x, x′, z, and E.

III. THE LESSONS LEARNED

The broad exploration followed by the down selection also allows highlighting the lessons we can learn at the end of the procedure. Indeed, among all the different explored configurations, only those where injection and acceleration procedures are uncoupled can provide accelerated beams meeting all the requirements. But this is not sufficient; special care to tackle directly the beam quality issue in the presence of a high charge is needed. These two topics will be discussed in the following.

A. Decoupling injection and acceleration processes

In view of designing an accelerator intended for reliable and steady operation, one would desire to opt for the simplest configuration, with the least complexity. The broad exploration presented in the previous section, however, shows that a certain degree of sophistication is necessary.

One would dream of a simple configuration composed by a single plasma stage illuminated by a single laser beam. This would allow saving the delicate operation of extraction of the particle beam from a plasma stage, transporting and then matching it to the next plasma stage, and saving the synchronization between multiple laser beams. Nevertheless, this seems not enough if a large acceleration field, a large charge, and a high beam quality are simultaneously desired. A more powerful driver will produce a higher accelerating field, and if it is also used to initiate particle injection, the beam charge can be high, but the beam quality will be intrinsically degraded at the start. The result is inversed for a less powerful driver. According to the previous section, only two separate stages could be a solution, one stage dedicated to the injection of a high-quality beam and the other exclusively to the acceleration to the desired energy. This is true for the LWFA schemes where the driver is a powerful laser and the injector is either another plasma stage or an rf one. For the PWFA scheme, the driver beam and the witness beam are produced quasi-independently thanks to the laser-comb configuration [23,24]. For the hybrid scheme with Trojan horse injection, the situation is inversed of that of the LWFA; the driver is a strong particle beam, and the injection is achieved with a moderate laser beam.

Uncoupling injection and acceleration is the master idea to obtain simultaneously a high beam charge and high beam quality, as two independent knobs are necessary for tuning two parameters. This is also imperative in the injection stage itself, where there is also a short acceleration to hundreds of MeV. We saw that, in the five injection techniques presented in Sec. II A, the three first ones applying the wave-breaking injection, shock-front injection, and ionization injection techniques do not allow one to obtain a big enough charge and a good enough beam quality at once. Only a refinement of those techniques, the ReMPI and down-ramp techniques, would allow achieving it.

The down-ramp injection is similar to the shock-front injection, but with a more sophisticated density transition, offering more parameters, i.e., more knobs, to adjust the beam charge and quality at once [32]. Figure 5 shows the down-ramp structure's details. We notice a smooth up ramp around 1 mm long followed by a density transition where electrons are injected. Finally, electrons are accelerated in a 2-mm-long plateau. Similar profiles have been obtained in hydrodynamics simulations of gas cells [55], proving that this kind of density profile is realistic. Variations in the gas cell give a great controllability of the beam parameters.

The ReMPI injection is based on the ionization injection, but with two or three laser beams instead of one [34,56]. The operating principle is sketched in Fig. 6. A single laser pulse delivered by a Ti:sapphire laser system is split into
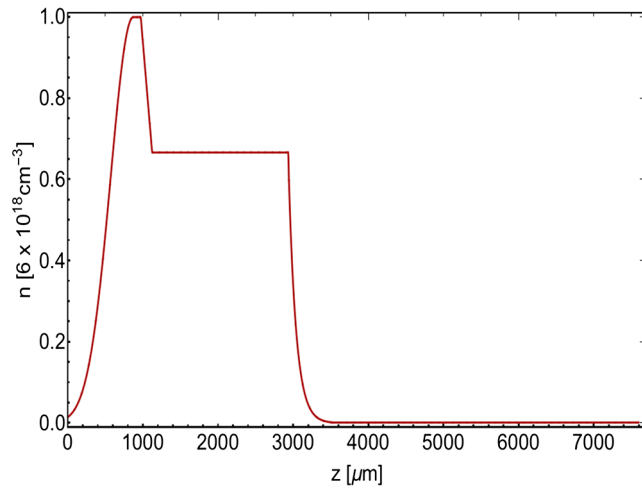
FIG. 5.   The longitudinal density profile used for the down-ramp injection scheme [32].

two pulses: A small fraction is used to ionize the plasma gas (preionized nitrogen 5+) in order to extract the electrons, and the remaining main part is time shaped as a train of four pulses which resonantly drive the wakefield without ionizing the plasma. The ionization pulse is frequency tripled by a nonlinear crystal and tightly focused behind the wake-driving pulse train. The extracted electrons are quickly trapped by the wake and accelerated up to the final energy of 150 MeV. A round beam is preferred for both the next optics and boosting stages and for minimizing beam loading in the current stage. But an intrinsic difficulty of the injection by ionization is the emittance increase in the direction of the laser polarization. This can be compensated by using the tail of the driving pulse, which is polarized perpendicularly to the ionization polarization, or else by using a third tiny laser beam with perpendicular polarization. No intrinsic time jitter will be present, as all the laser pulses are fractions of the single initial pulse.

The ReMPI technique can be used to accelerate electrons up to 5 GeV with all the required beam qualities with a single plasma stage and a single laser beam. However, this apparent simplicity must also include its part of sophistication. The plasma stage comprises two components, the first one dedicated to ionization is a helium gas cell doped
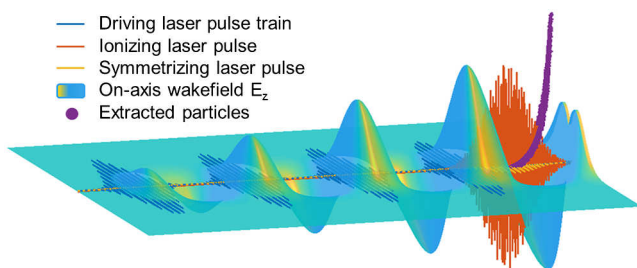

FIG. 6.   The three-laser system of the resonant multipulse injection and acceleration technique [56].

with argon preionized to the eighth level, and the second one dedicated to acceleration is a helium gas capillary where the gas density profile is radially parabolic. The laser beam must be split into a fourth harmonic ionization pulse and a driver pulse that must be decomposed into eight subpulses. Uncouple injection and acceleration are anyway necessary. The resulting higher complexity is, however, minimized in the present case, as shown in Ref. [56]. Instead of using two different lasers as in the two-color scheme, only one laser system is used, eliminating therefore synchronization-jitter issues. Because of the propagation of a pulse train in a nonuniform plasma, the evolution of the driver train is nontrivial and needs to be finely tuned to avoid too important depletion. Nevertheless, the resonant excitation of a pulse train induces a higher plasma wave amplitude than that coming from a single pulse. Numerical simulations showed that this acceleration scheme is stable, and the generation of laser pulse trains has been already demonstrated experimentally.

B. High beam quality and high beam charge issues

The demand of high beam quality, namely, low emittance and low energy spread, certainly requires great effort to achieve. This is true everywhere in the chain of beam injection, acceleration, and transport. Failing in minimizing the beam phase-space size at a given location will be very hard to compensate downstream. When the demand of high charge comes in addition, space charge forces and beam-loading effects can no longer be neglected. Indeed, in the best case, we must imperatively take the charge into account, because the usual minimization methods at zero charge are useless, and in the worst case, it can even induce a beam quality degradation, making mandatory a delicate optimization procedure between high charge and high quality.

For an LPI, a fine balance between small emittance and high charge must be found, while for an LPAS, a fine compromise between small energy spread and high charge must be set.

An example can be seen with the LPI where the down-ramp injection technique mentioned above is applied. Typically, sharper down ramps lead to more captured charges but induce a larger emittance, an effect that is accentuated by a larger density jump before and after the ramp [57]. By tuning the sharpness of the ramp and the density jump, a compromise can be obtained so that the desired emittance and charge can be reached [32]. Although we can note that only a rough tuning is enough, this means that the presence of this kind of tuning on the experimental device later on is highly recommended, at least during the commissioning phases.

For the LPI where the ReMPI technique is applied, a suitable choice of the different laser pulses and the dopant gas must be carefully studied [56]. The number of ionized charges is higher for a stronger ionization laser pulse, but it

will also induce a bigger emittance. Fortunately, the latter can be lowered with a smaller laser focal spot and a lower gas ionization potential. The driver laser must be intense enough to capture the ionized charges and to induce a wakefield strong enough for accelerating electrons to the wanted energy, but its energy cannot exceed the ionization potential in order not to ionize the gas. We can see that the ionization and driver laser strengths a_{0i} and a_{0d}, their focal spot sizes w_{0i} and w_{0d}, the number of driver subpulses, and the gas ionization potential U_i intimately interfere together. Only a judicious choice of these parameters can lead to the right compromise allowing one to reach all the contradictory objectives simultaneously.

For the LPAS under the quasilinear acceleration regime, except beam matching to a transversal focusing channel, no other action is required for preserving emittance. Particular attention should be rather dedicated to minimize the energy spread due to different accelerating field amplitudes seen by different parts of the beam during the acceleration process. It is well known that in the case where the charge is negligible, the phase dependence of the wakefield along the bunch phase is the main source of energy spread; therefore, reducing the bunch length as much as possible results in minimizing the energy spread. When the charge is substantial, however, the induced beam-loading field is no more negligible and can partly compensate the longitudinal variation of the wakefield. It was then suggested to impose a specific shape, triangular, for example, to the bunch longitudinal density in order to minimize the energy spread [58], but this is hard to achieve, especially in the case where the input beam is coming from the LPI where many other constraints must already be satisfied. It is noted in Ref. [41] that, while the energy spread induced by the wakefield depends directly on the bunch length, the energy spread induced by the beam-loading field depends on the beam radius. It is because the wakefield is almost constant on the

small transversal extent of the beam size, while the field generated by the beam itself directly depends on its radial profile. Therefore, for a given charge and a given beam radius, there exists a bunch length where the two effects compensate each other the best, minimizing consequently the energy spread. Figure 7(a) shows this bunch length in the case of the LPAS of scheme 2, which is not zero contrarily to the case of zero charge.

For some applications like the free electron laser, it is also necessary to minimize the slice energy spread, i.e., that of particles at the same longitudinal position but different radial positions. The relative slice energy spread, i.e., relative to the average beam energy, depends on the latter, which increases with the plasma density n_p, and on the beam-loading field which is proportional to $\sqrt{n_p}$ and decreases with the laser strength a_0 [41]. Hence, by tuning jointly a_0 and n_p, the slice energy spread can be minimized [Fig. 7(b)].

Another technique which has been shown to successfully minimize the energy spread consists in splitting the acceleration process into two plasma stages joined by a magnetic chicane. In this way, the energy chirp accumulated in the first stage is inverted in the chicane and can then be effectively compensated for in the second stage [45]. The principle of this technique is sketched in Fig. 8. This method is ideal for a linear chirp like that induced by the accelerating fields in the blowout regime in the case of marginal beam loading.

The principle of exploiting the beam loading itself by intentionally introducing it has been also exploited to drastically reduce the energy spread in the hybrid scheme under the blowout regime. As mentioned above, at the PPAS acceleration stage, a low emittance witness beam is generated by a small laser beam and accelerated to an energy high enough so that its emittance becomes hard to perturb. Then an escort beam is released by the upstream
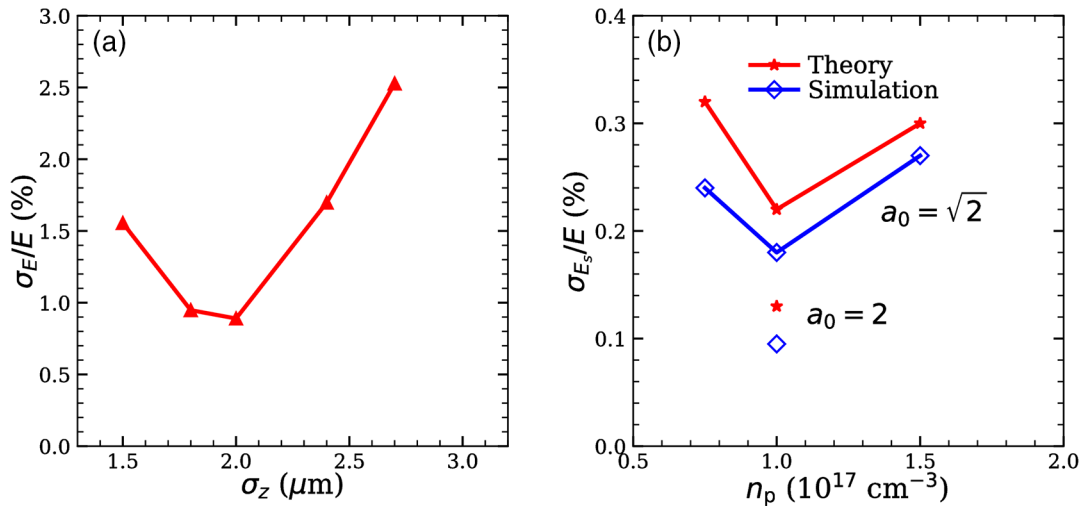

FIG. 7. (a) Minimization of energy spread with the bunch length. (b) Minimization of slice energy spread with the laser strength and the plasma density [41].
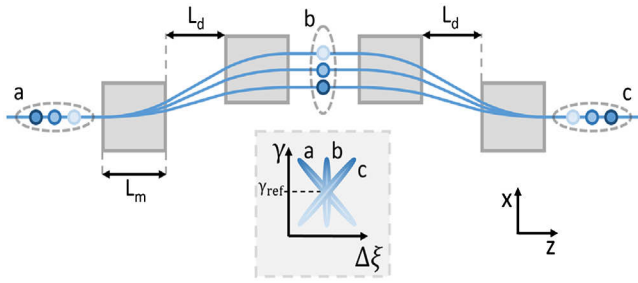
FIG. 8. Inversion of the beam energy chirp in a magnetic chicane between two identical LPAS. The longitudinal phase space is shown at the chicane (a) entrance, (b) middle, and (c) exit. Darker color means higher energy [45].

LPAS (in addition to the driver beam) that will completely overlap the witness bunch with a much higher charge. The expected effect of this escort beam is that, without perturbing the witness beam emittance, it will induce a beam-loading field strong enough to flatten the total accelerating field or even to reverse the wakefield when necessary, so as to avoid energy spread increase or even to reduce it [53]. Simulations for a low charge witness beam has demonstrated the efficiency of such a method, which should also work with a higher charge.

Once the optimization techniques have demonstrated their ability to offer charge, emittance, and energy spread as required, the work is not finished. In contrast to a physics experiment, obtaining good beam quality in the plasma stage is not enough; we also have to preserve this quality during beam extraction from or injection to a plasma stage, as well as transport between two plasma stages or from the plasma stage toward the final user.

IV. BEAM EXTRACTION, INJECTION, AND TRANSPORT ISSUES

As for any conventional linear accelerator (linac), it is necessary to design and optimize the transport lines between two accelerator stages and toward the final user. We have seen in the above sections that transport lines could be requisitioned to play an active role in the longitudinal phase space, either by compressing the bunch length in the rf injector or else to dechirp the beam energy between two accelerator stages.

We will focus here on the issues in the transverse phase space and, more specifically, the preservation of emittance in the presence of beam loading. It is very well known that extracting or injecting into a LPAS without particular care can lead to a significant increase of the emittance [59,60]. Despite that and despite many theoretical studies suggesting different plasma ramp density profiles [61,62,63], it is not clear which emittance will grow in which situation and what is the procedure to mitigate it in a practical case where beam loading cannot be neglected.

A thorough study with a consistent formalism has been undertaken, allowing one to clearly establish the circumstances of emittance growth in a transport line, the parameters governing this growth, and, thus, to determine the location where such parameters should be minimized [64]. Two types of emittance are considered: the phase emittance defined in the (x, p_x) space and the trace emittance in the (x, x') space, where x, p_x, and x' are the particle position, momentum, and momentum angle, respectively. Although the two first coordinates are the Hamiltonian conjugates, the phase emittance does not have any practical meaning and is generally useless. In contrast, the trace emittance directly characterizes the beam size and divergence. These two emittances are more different for a larger energy spread and larger beam divergence, but they are linked together and are, in particular, equal at every beam waist, which is generally in quadrupoles or in long enough drifts. Hence, the growth of both emittances should be mitigated. Outside the plasma, in a transport line, the phase emittance increases in a free drift, while the trace emittance remains constant, and inversely in a focusing element. These increases are due to (i) two parameters in the transfer line: the drift length and the focusing strength, and (ii) three parameters at the plasma exit: the (trace) emittance, the energy spread, and the Twiss parameter γ. Notice that the latter is constant in a free drift and is very large in the plasma stage, because the huge focusing forces therein impose a tiny beam size.

It is therefore straightforward to state that, in order to mitigate emittance growth when extracting the beam from a plasma stage [64], (i) The emittance and the energy spread should be minimized within the plasma stage exclusively; (ii) the Twiss parameter γ should be minimized at the plasma exit exclusively, with a down ramp or a passive plasma lens, for example, while ensuring that the latter will not induce themselves a too large emittance growth; and (iii) the total drift length (especially the first drift at the plasma exit) and the integrated focusing force should be minimized within the transport line.

It is important to stress that the minimization of these parameters at those three components guarantees a minimum emittance growth. This can be done at best at each component independently, without minding about what can be done at the next one. If, however, it is not properly done at a given stage, it can no longer be compensated elsewhere downstream.

In order to minimize γ, it is enough to tune the length of the plasma down ramp, whatever its shape. For the scheme-2 LPAS exit at 5 GeV, different types of down-ramp density profiles have been tested, exponential, linear, and Gaussian, and they all prove to be equally efficient for about the same global length, so that γ can be decreased from 400 to 80 m^{-1}, with a negligible increase in emittance. On the injection side at 150 MeV, if the plasma hard edge is adopted, the requested $\sim \mu$m beam size at the entrance will impose a large focusing force from the transport line, implying a big emittance degradation there. An up ramp

with about the same length as that of the down ramp allows relaxing the matched beam size by a factor of 10.

For the LPI where the blowout regime is applied, γ is much bigger, and a down ramp does not help to decrease it enough, the use of a passive plasma lens is necessary in addition. In the case of the LPI studied with the ReMPI technique, γ is decreased from 5000 to 1700 m^{-1} by the down ramp and then to 130 m^{-1} by the plasma lens. In the case of the down-ramp injection technique, these numbers at the plasma exit are, respectively, 14000, 4000, and 182 m^{-1}.

Such low γ will greatly help to lower the needed focusing strength in the transport lines. For a given input beam, the mission of the transport line is to shape a beam at the exit with a given beam size and divergence as requested by the next plasma stage or the final user, with the smoothest focusing. That means three constraints in each transverse direction and, thus, six quadrupoles are needed. We recommend not to implement more quadrupoles unless a longer line is needed for including diagnostics or chicanes. An optimized line called LETL is shown in Fig. 9(left), linking the ReMPI LPI to the scheme-2 LPAS, where the beam sizes are of the same order at the entrance and exit. The total length is 0.7 m, and six permanent quadrupole magnets are used. The emittance has been doubled, from 0.3 to 0.6 mm mrad, mainly due to longitudinal space charge forces within the 30 pC short bunch of 8 fs at this low energy of 150 MeV. The optimized HETL (high-energy transfer line) is shown in Fig. 9(right), linking the scheme-2 LPAS to the FEL application, where, as expected, the beam size at the exit is much bigger than at the entrance. The total length is 4 m; two permanent magnets and four electromagnets are used. The emittance increase is 10%.

These results are encouraging, as they demonstrate the concepts highlighted in the present studies for preserving emittance. Other studies are being performed to lengthen the transport lines in order to reserve a place for implementing diagnostic or driver removal devices and also to further limit the emittance growth.

V. SENSITIVITY TO ERRORS

For an accelerator that should routinely deliver a beam to users with high stability and high reliability, the study of sensitivity to different error sources is imperative. As for plasma-based accelerators, simulations are much more time consuming and physical phenomena significantly nonlinear, only small enough variations, whose effects are linear, will be considered, with the assumption that they can be later on combined quadratically. Errors are deviations from the nominal, ideal case, which is obtained after long and delicate optimizations. Since we cannot study large deviations where reoptimization is needed, the errors here must be understood in the sense of uncorrected jitters. The principle is to study separately, for each plasma stage or transport line, the effects of deviations of nominal parameters of the electron input beam, the laser, and the plasma, on the electron output beam parameters. This way, it will be possible in a next step to chain up the analysis to estimate the tolerances of each component back to the source when tolerances at the final application are requested.

First error analysis was done for the LPI with ReMPI and down-ramp injection techniques, the scheme-2, −3, and −4 LPAS, and the LETL and HETL. For all these stages, it is found that, in order not to significantly deteriorate the nominal performances, the position jitter of either the laser or the input electron beam should be a small fraction of their size. This not so surprising result shows, on the one hand, the consistency of the results obtained by our heavy simulations and, on the other hand, the stability of the selected configurations that do not feature any hidden error amplification.

More specifically for the LPI with the ReMPI technique, the driver-to-ionization laser distance is the most critical. However, we can see that 1 μm or 3 fs of jitter seems still acceptable, since it implies a 10% jitter on the exit beam energy, 15% on the emittance, and more than 10% on the energy spread. Indeed, these variations on these parameters at 150 MeV will be strongly damped by the acceleration to 5 GeV in the next accelerator stage.
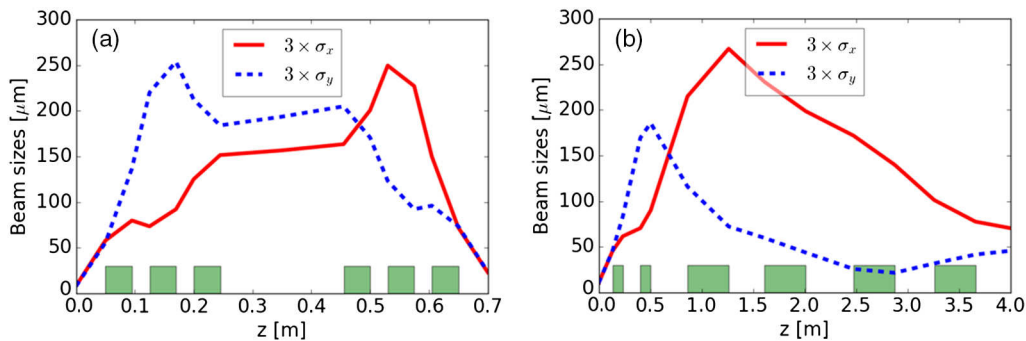

FIG. 9. Evolution of the beam size (3 sigmas) along the optimized LETL (a) and HETL (b). The quadrupoles are symbolized by the green boxes.

For the LPI with the down-ramp injection technique, the down-ramp length is crucial, as the sharpness of the down ramp is directly related to the amount of charges injected into the bubble. Nevertheless, our analysis shows that small changes (5%) in the ramp length lead to similar changes in the beam parameters, amplified by a factor from 1 to 2.

For the scheme-2 LPAS, sensitivity to all types of errors remains at a small level, except for the cylindrical asymmetry. An amount of laser energy as small as 1% in the nonaxial symmetry modes is enough to increase the emittance by an order of magnitude. Note also that, in such a case, the electron beam has an angle of 0.4 mrad with the laser one. Clearly, particular attention should be paid to compensate this aspect. Besides, a laser-electron delay of 2 fs or 1% plasma density fluctuations induce 1% energy variation.

For the scheme-3 LPAS, variations of 10%–20% of the input parameters return a beam similar to the nominal one. The sensitivity to cylindrical symmetry break is suspected but the code used (QFluid) does not allow one to simulate this correctly: An offset of 1.5 μm in the position and 20 μrad in the angle of the input electron beam would produce 50% variation of emittance change. It appears also that the final slice energy spread is very sensitive to laser and plasma parameters.

For the scheme-4 LPAS, sensitivity studies to variations in the initial beam offsets (transverse and longitudinal) as well as to variations in the shape of the ramps have been performed with the WAKE-T code [65]. From the considered parameters, the electron beam longitudinal offsets at injection appear to be the most critical. In the particular working point studied, a maximum longitudinal offset of 0.3 fs, far beyond the state of the art, is required to keep the energy spread variations under 10%. In order to achieve this degree of precision, this acceleration scheme might have to be coupled with the timing jitter correction concept presented in Ref. [66]. It should also be noted, however, that the energy spread requirements in Table I are still met for longitudinal offsets in the ±5 fs range.

The PWFA schemes are known to be subject to timing jitter between the drive beam and the witness beam, which can induce deterioration of the energy spread downstream, but different techniques, as, for example, the passive bunching technique [67], allow one to minimize this effect.

For the transport lines, the effect of quadrupole misalignment on the final beam position is the most critical. It is stronger for permanent magnets and for the transport line toward the FEL application, because it is proportional to $K\sqrt{\beta_Q \beta_f}$ (the quadrupole strength and the Twiss parameters at the respective locations). This effect relative to the final beam size is proportional to $K\sqrt{\beta_Q/\varepsilon}$ (ε is the nonnormalized trace emittance). It is therefore stronger at 5 GeV than at 150 MeV. As a consequence, if we want the beam position jitter to be a fraction of the beam size at the exit, then the tolerance on the permanent magnet position jitter should be less than 1 μm in the 150 MeV LETL and a factor of 2 or 3 smaller in the 5 GeV HETL. Studies of an efficient damping system, an antivibration girder, or/and a high-performance feedback for these permanent magnets are definitely essential.

VI. SPECIFICATIONS OF PLASMA AND LASER PARAMETERS

Many configurations composed of different injection or acceleration schemes, where different injection and acceleration techniques have been applied, are studied in detail and optimized in view of the required high charge, high energy, and high beam quality. The most suitable configurations regarding the requirements have been selected for start-to-end simulations: single LPAS with ReMPI injection technique followed by quasilinear acceleration to 5 GeV, passive plasma lens, and HETL; LPI with ReMPI injection technique to 150 MeV, passive plasma lens, LETL, LPAS under quasilinear acceleration to 5 GeV, and HETL; RFI with rf and magnetic bunching to 540 MeV, LPAS under quasilinear acceleration to 5 GeV, and HETL; RFI with rf and magnetic bunching to 240 MeV, LPAS under two sections separated by a magnetic chicane, under blowout acceleration to 5 GeV; RFI with COMB technique to 500 MeV, PPAS under weakly nonlinear acceleration to 1 GeV, and HETL.

From that, the specifications for the laser and plasma physical parameters can be determined.

For the single-LPAS configuration, the required laser parameters are 872 TW, E = 51 J, and strength $a_0 = 0.64$ (split into three beams as explained above); and the plasma comprises two parts: $He + Ar^{8+} (50\%)$ and then He radially parabolic, uniform density $n_0 = 2 \times 10^{17}$ cm^{-3}, 250 mm long, 10 mm down ramp, and a 10 mm passive plasma lens, $n_0 = 1.4 \times 10^{16}$ cm^{-3}.

For the LPI at 150 MeV, in the case of ReMPI, the required laser parameters are P = 200 TW, E = 5 J, and strength $a_0 = 1$ (split into three beams as explained above); and for the plasma: N^{5+}, uniform density $n_0 = 1 \times 10^{18}$ cm^{-3}, 3.5 mm long, 1 mm down ramp, and a 3 mm passive plasma lens, $n_0 = 1.4 \times 10^{16}$ cm^{-3}. In the case of down-ramp injection, the laser parameters are much relaxed: P = 35 TW, E = 1 J, and $a_0 = 1.8$; but the plasma is more complex: $n_0 = 6 \times 10^{18}$ cm^{-3}, a density increase then decrease with a plateau between, on a few 0.1 mm, 0.15 mm down ramp at the exit, and a 4 mm passive plasma lens with $n_0 = 1 \times 10^{16}$ cm^{-3}.

For the LPAS under quasilinear acceleration to 5 GeV, the required laser parameters are P = 400 TW, E = 60 J, and $a_0 = 2.42$; and for the plasma: radially parabolic, longitudinally uniform, 300–500 mm long, $n_0 = 1$ to 2×10^{17} cm^{-3}, and entrance and exit ramps $\sim$20 mm.

For the LPAS under blowout acceleration to 5 GeV, the needed laser is more powerful: P = 750 TW, E = 40 J,

and $a_0 = 3$; and for the plasma that is split in two parts, each one radially parabolic, longitudinally uniform, 80 mm long, and $n_0 = 1 \times 10^{17}$ cm^{-3}.

In summary, keep in mind that the plasma stage has a density around 10^{17} cm^{-3} and should be equipped so that the plasma depth and the ramp lengths can be tuned, while the needed laser power is generally well under the petawatt but with a high energy of tens of joules.

VII. CONCLUSIONS

Substantial efforts have been deployed to design a plasma-based accelerator capable of delivering a stable beam with simultaneously high charge, high energy, and high beam quality. Many different injection and acceleration schemes and techniques have been studied in detail and optimized thoroughly.

Innovative methods have been developed to tackle the two aspects of beam quality, i.e., emittance and energy spread, in the presence of space charge and beam loading. In the injection stage, at the beam generation source, emittance minimization should be the object of utmost care, because, unless charge losses are accepted, the emittance cannot be improved afterward. In the acceleration stage, provided that the transverse phase space is properly matched to minimize emittance growth, special efforts should be then devoted to minimize energy spread. The issue of emittance preservation has been examined and solved for extracting and injecting the electron beam from and to a plasma stage, as well as for transporting it between two plasma stages or toward the final application, in the presence of space charge and beam-loading effects.

As for a conventional accelerator, start-to-end simulations have been performed and sensitivity to errors analyzed. All these optimization and simulation efforts allowed us to show that solutions do exist fulfilling the most challenging requirements such as those of a hard-x-ray FEL, and, among them, the acceleration in quasilinear regime proved to be highly robust. Other acceleration techniques like ReMPI or those using a magnetic chicane or an additional escort beam are also highly promising. In all cases, further improvements are still possible. They are anyway desirable in order to widen the margin as regard to requirements.

Furthermore, the hard points that deserve special attention and the needs in terms of laser and plasma systems are highlighted. In the plasma stages, the break of cylindrical symmetry appears to be the most critical, together with the delay between the laser and the electron beams. In the transport lines, the vibrations of the permanent quadrupole magnets should be drastically damped. The laser needs not to be very powerful but highly energetic. The plasma cells should be equipped so that the transverse profile and the ramp lengths could be easily tuned.

Other important aspects, not discussed here because out of the scope of this article, remain to be considered. The compactness, one representative benefit of plasma acceleration compared to rf acceleration, should be assessed. It can be roughly estimated that the acceleration schemes explored here can potentially induce a factor of 5–10 gain in the floor footprint. For the moment, only criteria about beam parameters are taken into account, but in fine, the overall size of the accelerator should be in addition considered in the selection of the best configurations. Typically, an rf injector can look bulky compared to a laser-plasma injector, but the new X-band technology can help to limit the linac size to less than 10 m, which is to be compared to the required floor space of a laser system. The repetition rate and the energy efficiency should also be assessed. In the results reported above, an up to 60 J laser is required for producing a good quality beam at 30 pC and 5 GeV, which is a very poor energy transfer from the laser to the beam. Future studies should also aim at optimizing laser power and energy in addition to beam quality criteria.

ACKNOWLEDGMENTS

[1] E. Esarey, C. B. Schroeder, and W. P. Leemans, Physics of laser-driven plasma-based electron accelerators, Rev. Mod. Phys. **81**, 1229 (2009).

[2] I. Blumenfeld, C. E. Clayton, F.-J. Decker, M. J. Hogan, C. Huang, R. Ischebeck, R. Iverson, C. Joshi, T. Katsouleas, N. Kirby, W. Lu, K. A. Marsh, W. B. Mori, P. Muggli, E. Oz, R. H. Siemann, D. Walz, and M. Zhou, Energy doubling of 42 GeV electrons in a metre-scale plasma wakefield accelerator, Nature (London) **445**, 741 (2007).

[3] S. P. D. Mangles, C. D. Murphy, Z. Najmudin, A. G. R. Thomas, J. L. Collier, A. E. Dangor, E. J. Divall, P. S. Foster, J. G. Gallacher, C. J. Hooker, D. A. Jaroszynski, A. J. Langley, W. B. Mori, P. A. Norreys, F. S. Tsung, R. Viskup, B. R. Walton, and K. Krushelnick, Monoenergetic beams of relativistic electrons from intense laser–plasma interactions, Nature (London) **431**, 535 (2004).

[4] C. G. R. Geddes, C. Toth, J. van Tilborg, E. Esarey, C. B. Schroeder, D. Bruhwiler, C. Nieter, J. Cary, and W. P. Leemans, High-quality electron beams from a laser wakefield accelerator using plasma-channel guiding, Nature (London) **431**, 538 (2004).

[5] J. Faure, Y. Glinec, A. Pukhov, S. Kiselev, S. Gordienko, E. Lefebvre, J.-P. Rousseau, F. Burgy, and V. Malka, A laser–plasma accelerator producing monoenergetic electron beams, Nature (London) **431**, 541 (2004).

[6] K. Nakamura, B. Nagler, Cs. Tóth, C. G. R. Geddes, C. B. Schroeder, E. Esarey, W. P. Leemans, A. J. Gonsalves, and S. M. Hooker, GeV electron beams from a centimeter-scale channel guided laser wakefield accelerator, Phys. Plasmas **14**, 056708 (2007).

[7] X. Wang *et al.*, Quasi-monoenergetic laser-plasma acceleration of electrons to 2 GeV, Nat. Commun. **4,** 1988 (2013).

[8] H. T. Kim, K. H. Pae, H. J. Cha, I. J. Kim, T. J. Yu, J. H. Sung, S. K. Lee, T. M. Jeong, and J. Lee, Enhancement of Electron Energy to the Multi-GeV Regime by a Dual-Stage Laser-Wakefield Accelerator Pumped by Petawatt Laser Pulses, Phys. Rev. Lett. **111,** 165002 (2013).

[9] W. P. Leemans, A. J. Gonsalves, H.-S. Mao, K. Nakamura, C. Benedetti, C. B. Schroeder, C. Tóth, J. Daniels, D. E. Mittelberger, S. S. Bulanov, J.-L. Vay, C. G. R. Geddes, and E. Esarey, Multi-GeV Electron Beams from Capillary-Discharge-Guided Subpetawatt Laser Pulses in the Self-Trapping Regime, Phys. Rev. Lett. **113,** 245002 (2014).

[10] A. J. Gonsalves *et al.*, Petawatt Laser Guiding and Electron Beam Acceleration to 8 GeV in a Laser-Heated Capillary Discharge Waveguide, Phys. Rev. Lett. **122,** 084801 (2019).

[11] B. S. Paradkar, B. Cros, P. Mora, and G. Maynard, Numerical modeling of multi-GeV laser wakefield electron acceleration inside a dielectric capillary tube, Phys. Plasmas **20,** 083120 (2013).

[12] W. Lu, M. Tzoufras, C. Joshi, F. S. Tsung, W. B. Mori, J. Vieira, R. A. Fonseca, and L. O. Silva, Generating multi-GeV electron bunches using single stage laser wakefield acceleration in a 3D nonlinear regime, Phys. Rev. Accel. Beams **10,** 061301 (2007).

[13] C. B. Schroeder, E. Esarey, C. G. R. Geddes, C. Benedetti, and W. P. Leemans, Physics considerations for laser-plasma linear colliders, Phys. Rev. Accel. Beams **13,** 101301 (2010).

[14] B. Hidding, G. Pretzler, J. B. Rosenzweig, T. Königstein, D. Schiller, and D. L. Bruhwiler, Ultracold Electron Bunch Generation via Plasma Photocathode Emission and Acceleration in a Beam-Driven Plasma Blowout, Phys. Rev. Lett. **108,** 035001 (2012).

[15] R. W. Assmann and J. Grebenyuk, Accelerator physics challenges towards a plasma accelerator with usable beam quality, in *Proceedings of the International Particle Accelerator Conference* (JACoW, Geneva, Switzerland, 2014), TUOBB01, https://doi.org/10.18429/JACoW-IPAC2014-TUOBB01.

[16] J. Cowley, C. Thornton, C. Arran, R. J. Shalloo, L. Corner, G. Cheung, C. D. Gregory, S. P. D. Mangles, N. H. Matlis, D. R. Symes, R. Walczak, and S. M. Hooker, Excitation and Control of Plasma Wakefields by Multiple Laser Pulses, Phys. Rev. Lett. **119,** 044802 (2017).

[17] A. Martinez de la Ossa, Z. Hu, M. J. V. Streeter, T. J. Mehrling, O. Kononenko, B. Sheeran, and J. Osterhoff, Optimizing density down-ramp injection for beam-driven plasma wakefield accelerators, Phys. Rev. Accel. Beams **20,** 091301 (2017).

[18] P. A. Walker *et al.*, Horizon 2020 EuPRAXIA design study, J. Phys. Conf. Ser. **874,** 012029 (2017).

[19] L. A. Gizzi, P. Koester, L. Labate, F. Mathieu, Z. Mazzotta, G. Toci, and M. Vannini, A viable laser for a user plasma accelerator, Nucl. Instrum. Methods Phys. Res., Sect. A **909,** 58 (2018).

[20] J. Zhu, R. W. Assmann, B. Marchetti, A. Feran Pousa, and P. A. Walker, Simulation study of an RF injector for the LWFA configuration at EuPRAXIA, in *Proceedings of the 9th International Particle Accelerator Conference, Vancouver, Canada* (JACoW Publishing, Geneva, Switzerland, 2018), THPAF032, https://doi.org/10.18429/JACoW-IPAC2018-THPAF032.

[21] L. Serafini and M. Ferrario, Velocity bunching in photo-injectors, *AIP Conf. Proc.* 581, 87 (2001).

[22] A. Giribono, A. Bacci, E. Chiadroni, A. Cianchi, M. Croia, M. Ferrario, A. Marocchino, V. Petrillo, R. Pompili, S. Romeo, M. R. Conti, A. R. Rossi, and C. Vaccarezza, RF injector design studies for the trailing witness bunch for a plasma-based user facility, Nucl. Instrum. Methods Phys. Res., Sect. A **909,** 229 (2018).

[23] M. Ferrario *et al.*, Laser comb with velocity bunching: Preliminary results at SPARC, Nucl. Instrum. Methods Phys. Res., Sect A **637,** S43 (2011).

[24] F. Villa *et al.*, Laser pulse shaping for high gradient accelerators, Nucl. Instrum. Methods Phys. Res., Sect. A **829,** 446 (2016).

[25] A. Beck, S. Y. Kalmykov, X. Davoine, A. Lifschitz, B. A. Shadwick, V. Malka, and A. Specka, Physical processes at work in sub-30 fs, PW laser pulse-driven plasma accelerators: Towards GeV electron acceleration experiments at CILEX facility, Nucl. Instrum. Methods Phys. Res., Sect. A **740,** 67 (2014).

[26] J. Derouillat, A. Beck, F. Pérez, T. Vinci, M. Chiaramello, A. Grassi, M. Flé, G. Bouchard, I. Plotnikov, N. Aunai, J. Dargent, C. Riconda, and M. Grech, SMILEI: A collaborative, open-source, multi-purpose particle-in-cell code for plasma simulation, Comput. Phys. Commun. **222,** 351 (2018).

[27] F. Massimo, A. F. Lifschitz, C. Thaury, and V. Malka, Numerical studies of density transition injection in laser wakefield acceleration, Plasma Phys. Controlled Fusion **59,** 085004 (2017).

[28] A. Lifschitz, X. Davoine, E. Lefebvre, J. Faure, C. Rechatin, and V. Malka, Particle-in-cell modelling of laser–plasma interaction using Fourier decomposition, J. Comput. Phys. **228,** 1803 (2009).

[29] T. L. Audet, P. Lee, G. Maynard, S. D. Dufrénoy, A. Maitrallain, M. Bougeard, P. Monot, and B. Cros, Gas cell density characterization for laser wakefield acceleration, Nucl. Instrum. Methods Phys. Res., Sect. A **909,** 383 (2018).

[30] J.-L. Vay, C. G. R. Geddes, E. Esarey, C. B. Schroeder, W. P. Leemans, E. Cormier-Michel, and D. P. Grote, Modeling of 10 GeV–1 TeV laser-plasma accelerators using Lorentz boosted simulations, Phys. Plasmas **18,** 123103 (2011).

[31] P. Lee, G. Maynard, T. L. Audet, B. Cros, R. Lehe, and J.-L. Vay, Optimization of laser-plasma injector via beam loading effects using ionization-induced injection, Phys. Rev. Accel. Beams **21,** 052802 (2018).

[32] T. Silva, A. Helm, J. Vieira, R. Fonseca, and L. O. Silva, On the use of the envelope model for down-ramp injection in laser-plasma accelerators, Plasma Phys. Controlled Fusion **62,** 024001 (2019).

[33] R. A. Fonseca *et al.*, OSIRIS: A three-dimensional, fully relativistic particle in cell code for modeling plasma based accelerators, Lect. Notes Comput. Sci. **2331,** 342 (2002).

[34] P. Tomassini, S. De Nicola, L. Labate, P. Londrillo, R. Fedele, D. Terzani, and L. A. Gizzi, The resonant multipulse ionization injection, Phys. Plasmas **24,** 103120 (2017).

[35] G. Toci, Z. Mazzotta, L. Labate, F. Mathieu, M. Vannini, B. Patrizi, and L. A. Gizzi, Conceptual design of a laser driver for a plasma accelerator user facility, Instruments **3,** 40 (2019).

[36] C. Benedetti, A. Sgattoni, G. Turchetti, and P. Londrillo, ALaDyn: A high-accuracy pic code for the Maxwell Vlasov equations, IEEE Trans. Plasma Sci. **36,** 1790 (2008).

[37] P. Tomassini and A. R. Rossi, Matching strategies for a plasma booster, Plasma Phys. Controlled Fusion **58,** 034001 (2016).

[38] R. Lehe, M. Kirchen, I. A. Andriyash, B. B. Godfrey, and J.-L. Vay, A spectral quasi-cylindrical and dispersion-free particle-in-cell algorithm, Comput. Phys. Commun. **203,** 66 (2016).

[39] P. Tomassini, D. Terzani, F. Baffigi, F. Brandi, L. Fulgentini, P. Koester, L. Labate, D. Palla, and L. A. Gizzi, High-quality 5 GeV electron bunches with the resonant multi-pulse ionization injection, Plasma Phys. Controlled Fusion **62,** 014010 (2019).

[40] X. Li, A. Mosnier, and P. A. P. Nghiem, Design of a 5 GeV laser–plasma accelerating module in the quasi-linear regime, Nucl. Instrum. Methods Phys. Res., Sect. A **909,** 49 (2018).

[41] X. Li, P. A. P. Nghiem, and A. Mosnier, Toward low energy spread in plasma accelerators in quasilinear regime, Phys. Rev. Accel. Beams **21,** 111301 (2018).

[42] E. Svystun, R. W. Assmann, U. Dorda, A. Feran Pousa, T. Heinemann, B. Marchetti, A. Martinez de la Ossa, P. A. Walker, M. K. Weikum, and J. Zhu, Beam quality preservation studies in a laser-plasma accelerator with external injection for EuPRAXIA, Nucl. Instrum. Methods Phys. Res., Sect. A **909,** 90 (2018).

[43] A. R. Rossi *et al.*, Stability study for matching in laser driven plasma acceleration, Nucl. Instrum. Methods Phys. Res., Sect. A **829,** 67 (2016).

[44] A. R. Rossi, V. Petrillo, A. Bacci, E. Chiadroni, A. Cianchi, M. Ferrario, A. Giribono, A. Marocchino, M. R. Conti, L. Serafini, and C. Vaccarezza, Plasma boosted electron beams for driving free electron lasers, Nucl. Instrum. Methods Phys. Res., Sect. A **909,** 54 (2018).

[45] A. Feran Pousa, A. Martinez de la Ossa, R. Brinkmann, and R. W. Assmann, Compact Multistage Plasma-Based Accelerator Design for Correlated Energy Spread Compensation, Phys. Rev. Lett. **123,** 054801 (2019).

[46] X. L. Xu, J. F. Hua, Y. P. Wu, C. J. Zhang, F. Li, Y. Wan, C.-H. Pai, W. Lu, W. An, P. Yu, M. J. Hogan, C. Joshi, and W. B. Mori, Physics of Phase Space Matching for Staging Plasma and Traditional Accelerator Components Using Longitudinally Tailored Plasma Profiles, Phys. Rev. Lett. **116,** 124801 (2016).

[47] K. Floettmann, ASTRA–A space charge tracking algorithm, http://www.desy.de/~mpyflo/.

[48] M. Dohlus, A. Kabel, and T. Limberg, Efficient field calculation of 3D bunches on general trajectories, Nucl. Instrum. Methods Phys. Res., Sect. A **445,** 338 (2000).

[49] A. Marocchino, F. Massimo, A. R. Rossi, E. Chiadroni, and M. Ferrario, Efficient modeling of plasma wakefield acceleration in quasi-non-linear-regimes with the hybrid code Architect, Nucl. Instrum. Methods Phys. Res., Sect. A **829,** 386 (2016).

[50] F. Massimo, S. Atzeni, and A. Marocchino, Comparisons of time explicit hybrid kinetic-fluid code ARCHITECT for plasma wakefield acceleration with a full PIC code, J. Comput. Phys. **327,** 841 (2016).

[51] A. Martinez de la Ossa, R. W. Assmann, M. Bussmann, S. Corde, J. P. C. Cabadag, A. Debus, A. Döpp, A. Feran Pousa, M. F. Gilljohann, T. Heinemann, B. Hidding, A. Irman, S. Karsch, O. Kononenko, T. Kurz, J. Osterhoff, R. Pausch, and U. Schramm, Hybrid LWFAPWFA staging as a beam energy and brightness transformer: Conceptual design and simulations, Phil. Trans. R. Soc. A **377,** 20180175 (2019).

[52] A. Martinez de la Ossa, T. J. Mehrling, L. Schaper, M. J. V. Streeter, and J. Osterhoff, Wakefield-induced ionization injection in beam-driven plasma accelerators, Phys. Plasmas **22,** 093107 (2015).

[53] G. G. Manahan, A. F. Habib, P. Scherk, P. Delinikolas, A. Beaton, A. Knetsch, O. Karger, G. Wittig, T. Heinemann, Z. M. Sheng, J. R. Cary, D. L. Bruhwiler, J. B. Rosenzweig, and B. Hidding, Single-stage plasma-based correlated energy spread compensation for ultrahigh 6D brightness electron beams, Nat. Commun. **8,** 15705 (2017).

[54] C. Nieter and J. R. V. Cary, A versatile plasma simulation code, J. Comput. Phys. **196,** 448 (2004).

[55] O. Kononenko, N. C. Lopes, J. M. Cole, C. Kamperidis, S. P. D. Mangles, Z. Najmudin, J. Osterhoff, K. Poder, D. Rusby, D. R. Symes, J. Warwick, J. C. Wood, and C. A. J. Palmer, 2D hydrodynamic simulations of a variable length gas target for density down-ramp injection of electrons into a laser wakefield accelerator, Nucl. Instrum. Methods Phys. Res., Sect. A **829,** 125 (2016).

[56] P. Tomassini, D. Terzani, L. Labate, G. Toci, A. Chancé, P. A. P. Nghiem, and L. A. Gizzi, High quality electron bunches for a multi-stage GeV accelerator with the resonant multi-pulse ionization injection, Phys. Rev. Accel. Beams **22,** 111302 (2019).

[57] H. Ekerfelt, M. Hansson, I. G. González, X. Davoine, and O. Lundh, A tunable electron beam source using trapping of electrons in a density down-ramp in laser wakefield acceleration, Sci. Rep. **7,** 12229 (2017).

[58] T. Katsouleas, S. Wilks, P. Chen, J. Dawson, and J. Su, Beam loading in plasma accelerators, Part. Accel. **22,** 81 (1987).

[59] M. Migliorati, A. Bacci, C. Benedetti, E. Chiadroni, M. Ferrario, A. Mostacci, L. Palumbo, A. R. Rossi, L. Serafini, and P. Antici, Intrinsic normalized emittance growth in laser-driven electron accelerators, Phys. Rev. Accel. Beams **16,** 011302 (2013).

[60] M. Scisció, L. Lancia, M. Migliorati, A. Mostacci, L. Palumbo, Y. Papaphilippou, and P. Antici, Parametric study of transport beam lines for electron beams accelerated by laser-plasma interaction, J. Appl. Phys. **119,** 094905 (2016).

[61] K. Floettmann, Some basic features of the beam emittance, Phys. Rev. Accel. Beams **6,** 034202 (2003).

[62] I. Dornmair, K. Floettmann, and A. R. Maier, Emittance conservation by tailored focusing profiles in a plasma accelerator, Phys. Rev. Accel. Beams **18**, 041302 (2015).

[63] X. L. Xu, J. F. Hua, Y. P. Wu, C. J. Zhang, F. Li, Y. Wan, C.-H. Pai, W. Lu, W. An, P. Yu, M. J. Hogan, C. Joshi, and W. B. Mori, Physics of Phase Space Matching for Staging Plasma and Traditional Accelerator Components Using Longitudinally Tailored Plasma Profiles, Phys. Rev. Lett. **116**, 124801 (2016).

[64] X. Li, A. Chancé, and P. A. P. Nghiem, Preserving emittance by matching out and matching in plasma wakefield acceleration stage, Phys. Rev. Accel. Beams **22**, 021304 (2019).

[65] A. Feran Pousa, R. Assmann, and A. Martinez de la Ossa, WAKE-T: A fast particle tracking code for plasma-based accelerators, in *Proceedings of the of International Particle Accelerator Conference* (JACoW Publishing, Geneva, Switzerland, 2019), THPGW012, https://doi.org/10.18429/JACoW-IPAC2019-THPGW012.

[66] A. Feran Pousa, R. Assmann, R. Brinkmann, and A. Martinez de la Ossa, External injection into a laser-driven plasma accelerator with sub-femtosecond timing jitter, *J. Phys. Conf. Ser.* 874, 012032 (2017).

[67] L. Zhao, T. Jiang, C. Lu, R. Wang, Z. Wang, P. Zhu, Y. Shi, W. Song, X. Zhu, C. Jing, S. Antipov, D. Xiang, and J. Zhang, Few-femtosecond electron beam with terahertz-frequency wakefield-driven compression, Phys. Rev. Accel. Beams **21**, 082801 (2018).